Genetic deletion of vesicular glutamate transporter in dopamine neurons increases vulnerability to MPTP-induced neurotoxicity in mice

Hui Shen[a], Rosa Anna M. Marino[a], Ross A. McDevitt[a], Guo-Hua Bi[a], Kai Chen[a], Graziella Madeo[a], Pin-Tse Lee[a], Ying Liang[a], Lindsay M. De Biase[a], Tsung-Ping Su[a], Zheng-Xiong Xi[a], and Antonello Bonci[a,b,c,d,e,1]

[a]Intramural Research Program, National Institute on Drug Abuse, Baltimore, MD 21224; [b]Solomon H. Snyder Department of Neuroscience, Johns Hopkins University School of Medicine, Baltimore, MD 21205; [c]Department of Psychiatry, Johns Hopkins University School of Medicine, Baltimore, MD 21205; [d]Department of Neuroscience, Georgetown University Medical Center, School of Medicine, Washington, DC 20057; and [e]Department of Psychiatry, University of Maryland, School of Medicine, Baltimore, MD 21201

Edited by Reinhard Jahn, Max Planck Institute for Biophysical Chemistry, Goettingen, Germany, and approved October 18, 2018 (received for review January 26, 2018)

A subset of midbrain dopamine (DA) neurons express vesicular glutamate transporter 2 (VgluT2), which facilitates synaptic vesicle loading of glutamate. Recent studies indicate that such expression can modulate DA-dependent reward behaviors, but little is known about functional consequences of DA neuron VgluT2 expression in neurodegenerative diseases like Parkinson's disease (PD). Here, we report that selective deletion of VgluT2 in DA neurons in conditional VgluT2-KO (VgluT2-cKO) mice abolished glutamate release from DA neurons, reduced their expression of brain-derived neurotrophic factor (BDNF) and tyrosine receptor kinase B (TrkB), and exacerbated the pathological effects of exposure to the neurotoxin 1-methyl-4-phenyl-1,2,3,6-tetrahydropyridine (MPTP). Furthermore, viral rescue of VgluT2 expression in DA neurons of VglutT2-cKO mice restored BDNF/TrkB expression and attenuated MPTP-induced DA neuron loss and locomotor impairment. Together, these findings indicate that VgluT2 expression in DA neurons is neuroprotective. Genetic or environmental factors causing reduced expression or function of VgluT2 in DA neurons may place some individuals at increased risk for DA neuron degeneration. Therefore, maintaining physiological expression and function of VgluT2 in DA neurons may represent a valid molecular target for the development of preventive therapeutic interventions for PD.

Parkinson's disease | VgluT2 | MPTP | BDNF | midbrain DA neurons

Midbrain dopamine (DA) neurons play critical roles in control of motor, sensorimotor, and motivated behaviors (1, 2). Parkinson's disease (PD) is characterized by progressive degeneration of midbrain DA neurons with a marked loss of neurons in the substantia nigra pars compacta (SNc) and a modest loss in the ventral tegmental area (VTA) (3, 4). Classical motor symptoms such as postural instability, resting tremor, bradykinesia, and rigidity are generally attributed to DA neuron loss in the SNc, whereas motivational and affective impairments such as depression, anxiety, and apathy are associated with loss of DA neurons in both the VTA and SNc (5, 6). Despite extensive research in recent decades, our knowledge about the determinants of vulnerability of midbrain DA neurons in PD is still limited. Gaining novel insights into cellular and molecular factors that influence DA neuron susceptibility, or resilience to CNS insults, would have important implications for the development of neuroprotective strategies and the treatment of PD.

Recent studies indicate that a subpopulation of DA neurons in the VTA and SNc coexpress tyrosine hydroxylase (TH) and the vesicular glutamate transporter 2 (VgluT2) (7, 8) and corelease DA and glutamate in the striatum in rats and mice (9, 10). VgluT2 is the major subtype of VgluTs expressed in midbrain glutamatergic neurons (11). Selective deletion of the *SLC17A6* (VgluT2) gene in DA neurons decreased psychostimulant-induced hyperactivity (12, 13) and altered cocaine and sucrose self-administration (14), suggesting that glutamate release from DA neurons may play an important role in modulating reward-related behavior. In addition, selective deletion of VgluT2 from DA neurons may also affect DA neuron growth and survival in cell cultures and the developing brain (15). However, the role that VgluT2 expression plays in mediating DA neuron viability and resilience to neurotoxic insults in the adult brain has not been explored to our awareness.

Here, we generated conditional VgluT2-KO (VglutT2-cKO) mice in midbrain DA neurons and examined DA neuron growth and survival, glutamate release, and cellular and behavioral responses to exposure to the Parkinsonian neurotoxin 1-methyl-4-phenyl-1,2,3,6-tetrahydropyridine (MPTP). Our findings indicate that VgluT2 expression in DA neurons is neuroprotective against MPTP-induced DA neuron cell death and reveal a critical role for brain-derived neurotrophic factor (BDNF) and its receptor tyrosine receptor kinase B (TrkB) in shaping neuronal resilience.

Results

Absence of VgluT2 mRNA and Glutamate Release from DA Neurons in VgluT2-cKO Mice. To achieve selective deletion of VgluT2 from DA neurons, DAT-IRES-Cre heterozygous (Het) mice (in which

Significance

Parkinson's disease (PD) is a chronic dopamine (DA) neuron degenerative disorder. Little is known about factors that impact vulnerability of DA neurons to pathological insults. In this study, we found that vesicular glutamate transporter 2 (VgluT2) expression may play an important role in protecting DA neurons. Selective deletion of VgluT2 in DA neurons led to a significant reduction in expression of brain-derived neurotrophic factor and its receptor tyrosine receptor kinase B and a significant increase in DA neuron death caused by the neurotoxin 1-methyl-4-phenyl-1,2,3,6-tetrahydropyridine. Restoration of VgluT2 expression in DA neurons reversed these alterations. These findings suggest that reduced VgluT2 expression in DA neurons may constitute a risk factor in the development of PD and suggest potential therapeutic strategies for boosting resilience of DA neurons.

Author contributions: H.S., Z.-X.X., and A.B. designed research; H.S., R.A.M.M., R.A.M., G.-H.B., K.C., G.M., P.-T.L., Y.L., L.M.D.B., and T.-P.S. performed research; H.S., R.A.M.M., R.A.M., G.-H.B., P.-T.L., T.-P.S., Z.-X.X., and A.B. analyzed data; and H.S., Z.-X.X., and A.B. wrote the paper.

The authors declare no conflict of interest.

This article is a PNAS Direct Submission.

[1]To whom correspondence should be addressed. Email: antonello.bonci@nih.gov.

This article contains supporting information online at www.pnas.org/lookup/suppl/doi:10.1073/pnas.1800886115/-/DCSupplemental.

Published online November 15, 2018.

Cre recombinase is expressed under control of the DA transporter promotor) were crossed with VgluT2-floxed mice to generate VgluT2-cKO and VgluT2-Het control offspring (*Materials and Methods*). To confirm the loss of VgluT2 in DA neurons in VgluT2-cKO mice, we used RNAscope in situ hybridization (ISH) assays to quantify VgluT2, TH, and DAT mRNA expression in the midbrain. In the SNc and VTA, clear colocalization of VgluT2 and TH mRNA was observed in a subset of TH-positive neurons in VgluT2-Het control mice, but not in VgluT2-cKO mice (Fig. 1 *A*–*D* and *SI Appendix*, Fig. S1). Quantitative analysis revealed that approximately 20% of TH-immunopositive (TH^+) neurons in the VTA and SNc express VgluT2 in VgluT2-Het control mice (Fig. 1 *E* and *F*). In contrast, VgluT2-cKO mice showed a significant reduction in TH^+-$VgluT2^+$ neurons, with fewer than 3% of TH^+ neurons displaying such colocalization (SNc, $P < 0.01$; VTA, $P < 0.01$; Fig. 1*E*; SNc, $P < 0.001$; VTA, $P < 0.001$; Fig. 1*F*). No significant differences in total TH^+ neurons, TH^+-only neurons, or $VgluT2^+$-only neurons were observed between the two genotypes of mice. Examination of colocalization between VgluT2 and DAT in the midbrain confirmed that approximately 15% of DA neurons coexpressed VgluT2 and DAT in the SNc and VTA of Het mice (*SI Appendix*, Fig. S2 *A* and *B*), whereas only 2–5% of DA neurons showed such colocalization in VgluT2-cKO mice (*SI Appendix*, Fig. S2 *C* and *D*).

To confirm elimination of functional VgluT2 from midbrain DA neurons, we used optogenetic approaches to stimulate VTA DA neuron terminals in the nucleus accumbens (NAc) and performed whole-cell patch-clamp recordings from postsynaptic medium spiny neurons (MSNs). Channel rhodopsin (ChR2) was expressed in midbrain DA neurons of VgluT2-cKO and VgluT2-Het mice via bilateral injections of cre-inducible AAV-DIO-ChR2-EYFP viral vector.

Eight weeks after virus injections, optical stimulation of VTA DA neuron terminals readily evoked excitatory postsynaptic currents (EPSCs) in all MSNs recorded from VgluT2-Het control mice (Fig. 1*G*), with mean inward current amplitude of 43.81 ± 7.27 pA (Fig. 1*H*) and latency of 2.65 ± 0.16 ms. Application of the AMPA receptor antagonist DNQX almost completely blocked these currents (Fig. 1*I*), confirming glutamate release from VTA DA neurons in these mice. In contrast, optical stimulation of DA neuron terminals in VgluT2-cKO mice did not produce any detectable currents in postsynaptic MSNs (Fig. 1 *G* and *H*), providing additional confirmation that functional VgluT2 is effectively eliminated from DAT-expressing DA neurons in these mice.

Deletion of VgluT2 in DA Neurons Enhances MPTP-Induced DA Neurotoxicity. We then examined whether VgluT2 expression in DA neurons influences the susceptibility of DA neurons to the neurotoxin MPTP. By using a well-described subacute MPTP dosing regimen (18 mg/kg × 4 with 2-h intervals), which leads to robust and reliable dopaminergic degeneration within a short period (1–2 wk) after MPTP administration (16), we found that systemic administration of MPTP produced significant DA neuron damage in the SNc and VTA of adult VgluT2-Het and VgluT2-cKO mice as assessed by reductions in the number of TH^+ cells at 14 d after MPTP treatment (Fig. 2 *A*–*D*). However, the loss of TH^+ cells was significantly greater in VgluT2-cKO mice than in VgluT2-Het mice (Fig. 2 *C* and *D*). The DA neurons in the SNc displayed higher vulnerability to MPTP than those in the VTA in Het control mice and VgluT2-cKO mice (Fig. 2 *C* and *D*), consistent with previous reports (17). To further explore possible links between VgluT2 expression and neuronal vulnerability, we quantified the percentage of surviving DA neurons that express VgluT2. Fig. 2*E* shows higher percentages of surviving DA neurons expressing VgluT2 in the SNc and VTA in MPTP-treated Het mice than in saline solution-treated Het mice, suggesting that those neurons that express VgluT2 are more likely to survive MPTP insult.

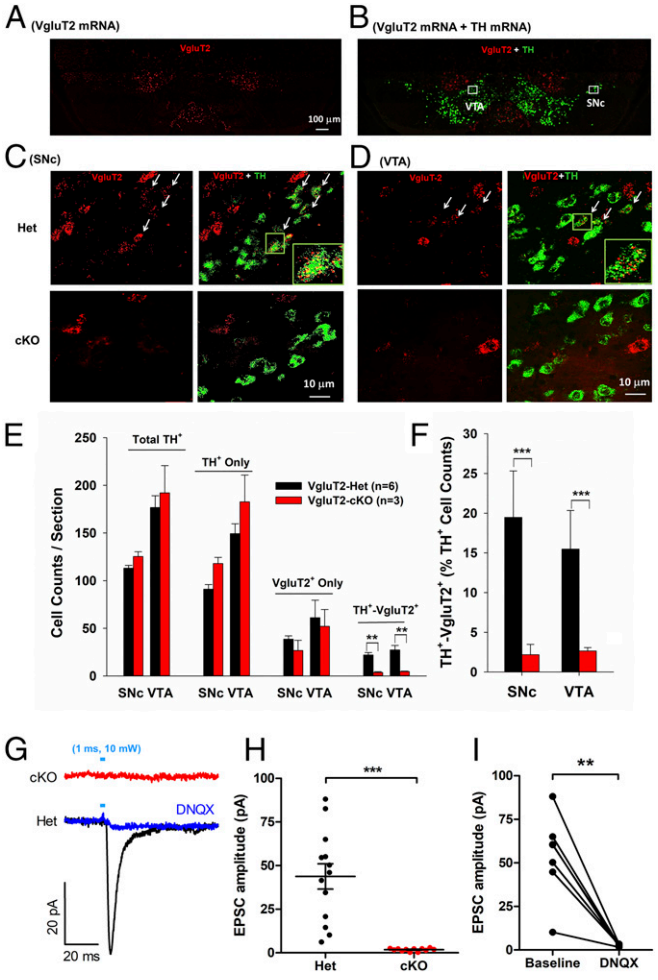

Fig. 1. Identification of VgluT2 expression in midbrain DA neurons in VgluT2-Het (Het) and VgluT2-cKO (cKO) mice. (*A* and *B*) Representative VgluT2-mRNA (red) and TH-mRNA (green) staining in a midbrain section under low magnification (10×) illustrates the two major areas of interest in this study, the VTA and SNc. (*C* and *D*) Representative confocal images of VgluT2 mRNA and TH mRNA staining in the SNc and VTA in Het and cKO mice. Insets (*Lower Right*) in images from the Het control mice are the magnified regions in the green boxes illustrating VgluT2 and TH colocalization in the same neurons. No VgluT2 mRNA was detected in TH^+ neurons in cKO mice. (*E*) Mean cell counts per section of total TH^+, TH^+-only, $VgluT2^+$-only, and TH^+-$VgluT2^+$ neurons in Het and cKO mice. There is a significant reduction in TH^+-$VgluT2^+$ cell counts between the two phenotypes of mice (*Right*; SNc, $t = 5.18$, $P < 0.01$; VTA, $t = 3.89$, $P < 0.01$). (*F*) cKO mice display a significant reduction in percentage of TH^+-$VgluT2^+$ neurons among total TH^+ neurons (SNc, $t = 4.42$, $P < 0.001$; VTA, $t = 3.77$, $P < 0.001$). (*G*) Electrophysiological recordings of EPSCs in striatal MSNs in brain slices illustrate optogenetic activation (1 ms of 473-nm, 10-mW laser) of DA neuron evoked EPSCs in Het but not in cKO mice. (*H*) Mean EPSC amplitudes in Het mice ($n = 13$ cells, three mice) and cKO mice ($n = 12$ cells, three mice). (*I*) Coadministration of DNQX, a selective AMPA receptor antagonist, blocked optical stimulation-evoked EPSCs in Het control mice [also see *G*; $n = 6$ cells, three mice; $^{**}P < 0.01$ and $^{***}P < 0.001$ vs. Het control mice (*E*, *F*, and *I*) or baseline (*H*)]. Data indicate mean ± SEM (*SI Appendix*, Figs. S1 and S2).

In addition to causing DA neuronal loss in the SNc and VTA, MPTP treatment also caused a significant reduction in the intensity of TH immunostaining (Fig. 2 *F* and *G*) throughout the striatum in both genotypes of mice, suggesting prominent degeneration of DA neuron terminals. Consistent with the analysis

NEUROSCIENCE

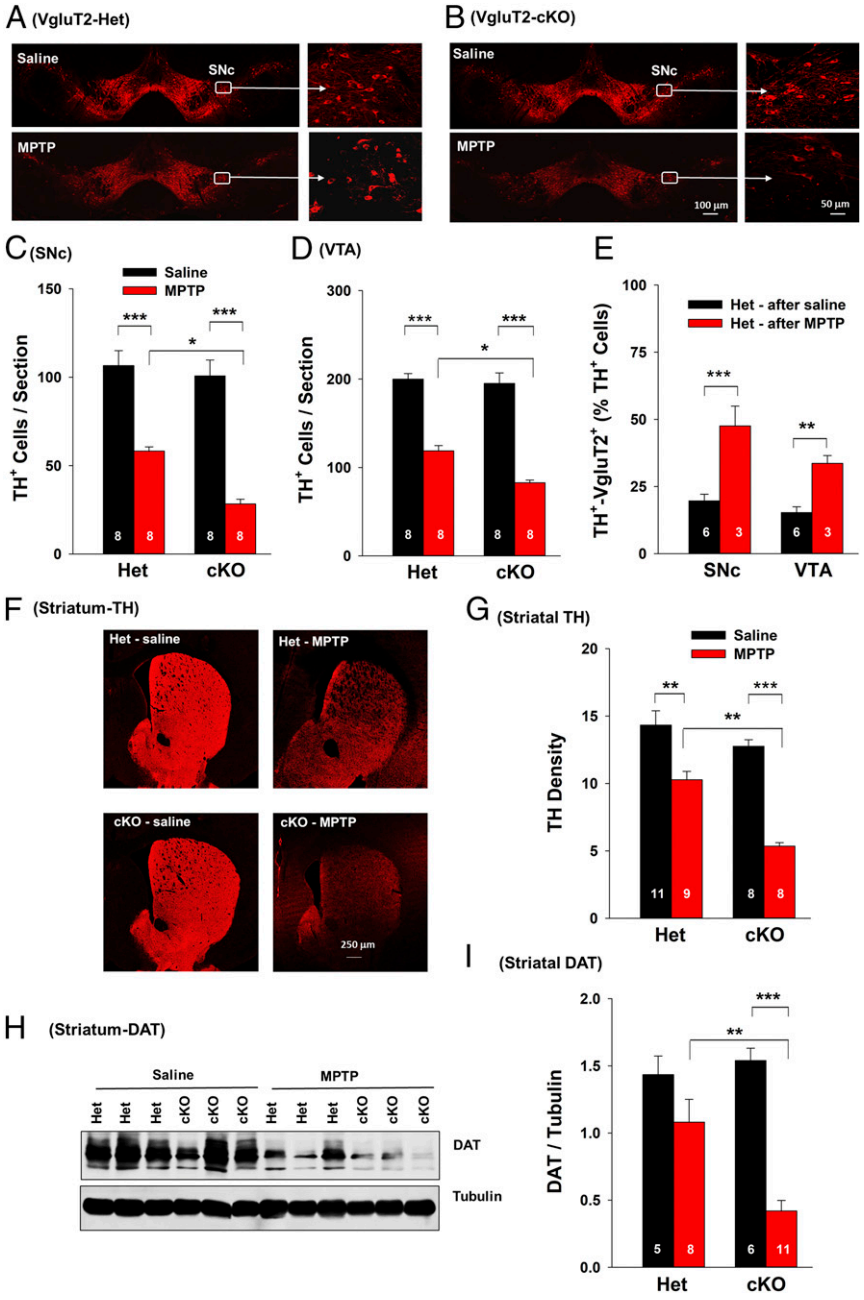

Fig. 2. MPTP-induced toxicity in DA neurons in Het and cKO mice. (*A* and *B*) Representative TH immunostaining images in Het and cKO mice 14 d after MPTP or saline solution treatment. (*C*) The mean TH^+ DA cell counts per section in the SNc (six brain sections per animal, eight animals per genotype). Two-way ANOVA revealed MPTP treatment main effect ($F_{1,28} = 127.81$, $P < 0.001$), genotype main effect ($F_{1,28} = 14.58$, $P < 0.001$), and treatment × genotype interaction ($F_{1,28} = 4.68$, $P < 0.05$). (*D*) The mean TH^+ DA cell counts per section in the VTA. Two-way ANOVA revealed MPTP treatment main effect ($F_{1,28} = 199.6$, $P < 0.001$), genotype main effect ($F_{1,28} = 7.86$, $P < 0.01$), and treatment × genotype interaction ($F_{1,28} = 6.13$, $P < 0.05$). (*E*) $VgluT2^+$-TH^+ neuron counts illustrating that more DA neurons expressed VgluT2 in the remaining surviving DA neurons in Het mice after MPTP administration than in Het mice after saline solution treatment. (*F*) Representative TH immunostaining images in the striatum. (*G*) Mean TH immunostaining density. Two-way ANOVA revealed MPTP treatment main effect ($F_{1,32} = 55.09$, $P < 0.001$), genotype main effect ($F_{1,32} = 17.68$, $P < 0.001$), and treatment × genotype interaction ($F_{1,32} = 4.74$, $P < 0.05$). (*H*) Original Western blot results. (*I*) Mean density of DAT band in the striatum. Two-way ANOVA revealed MPTP treatment main effect ($F_{1,28} = 18.49$, $P < 0.001$), genotype main effect ($F_{1,28} = 0.46$, $P > 0.05$), and treatment × genotype interaction ($F_{1,28} = 8.16$, $P < 0.01$) (*$P < 0.05$, **$P < 0.01$, and ***$P < 0.001$ vs. saline solution group or Het control mice; *SI Appendix*, Figs. S3 and S7).

of TH^+ cells in the midbrain, these MPTP-induced reductions in striatal TH staining were more extensive in VgluT2-cKO mice than in VgluT2-Het control mice. No significant change in VgluT2 immunostaining was observed in the striatum following MPTP treatment in mice of both genotypes (*SI Appendix*, Fig. S3 *A* and *B*). This may be related to the fact that the striatum receives VgluT2-expressing glutamatergic projections from multiple brain regions and multiple phenotypes of VgluT2-expressing neurons (11, 18). Afferents from VgluT2-expressing DA neurons represent only a small subset of the total number of VgluT2-positive terminals in striatum, which may obscure loss of a comparatively small number of $VgluT2^+$ terminals from midbrain DA neurons.

To confirm these histological findings, we used Western blot assays to measure DAT protein levels in the striatum (Fig. 2*H* and *SI Appendix*, Fig. S3*C*). Treatment with MPTP significantly decreased DAT levels in both genotypes of mice when measured at 14 d after MPTP administration (Fig. 2*I*). Again, MPTP-induced reductions in striatal DAT protein levels were more severe in VgluT2-cKO mice than in VgluT2-Het control mice. Together, these findings indicate that the loss of VgluT2 expression in DA neurons leads to more severe MPTP-induced DA neuron cell death and DA terminal degeneration, suggesting a critical role for this transporter in influencing DA neuron viability and susceptibility to pathological insults.

Deletion of VgluT2 in DA Neurons Enhances MPTP-Induced Behavioral Impairment. To determine whether increased DA neuron damage in VgluT2-cKO mice resulted in significant changes at the behavioral level, we examined MPTP-induced impairments in several commonly used tests of locomotor function in rodent models of PD (19). In the highly sensitive parallel rod floor test, animals were placed on an elevated horizontal ladder and trained to cross the device while a computer recorded paw slipping. MPTP treatment produced a significant increase in foot fault counts in VgluT2-cKO mice compared with VgluT2-Het controls (Fig. 3*A*). In the rotarod task, used to assess motor coordination and learning, although both strains of mice showed a significant decrease in the latency to fall after MPTP treatment, the reduction was greater in VgluT2-cKO mice than in VgluT2-Het control mice (Fig. 3*B*). We also examined the effects of MPTP treatment on open-field locomotion. MPTP treatment produced impaired vertical (Fig. 3*C*) and horizontal (Fig. 3*D*) locomotor activity, with reductions being more pronounced in VgluT2-cKO mice than in control mice. Together, these findings indicate that exposure to MPTP produced more severe locomotor deficits in mice lacking VgluT2 in DA neurons than in the VgluT2-Het control mice.

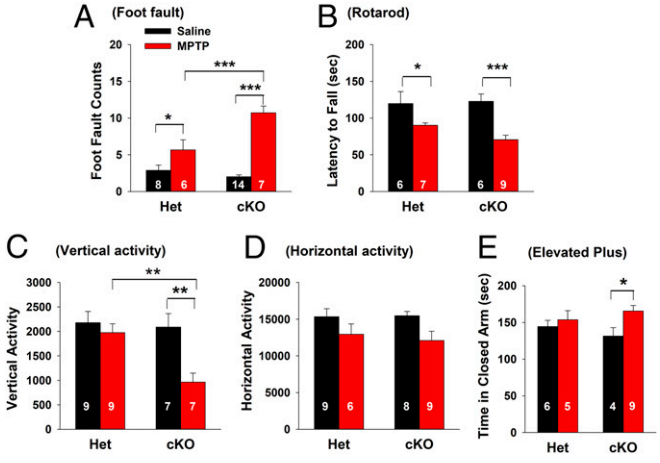

Fig. 3. MPTP-induced locomotor impairments in Het and cKO mice. (*A*) Parallel rod floor (foot fault) test results: MPTP produced a significant increase in foot fault counts in the cKO mice compared with the Het control mice (two-way ANOVA, MPTP treatment, $F_{1,31} = 62.57$, $P < 0.001$; genotype, $F_{1,31} = 8.23$, $P < 0.01$; treatment × phenotype interaction, $F_{1,31} = 16.57$, $P < 0.001$). (*B*) Rotarod test results: MPTP produced significant impairment in rotarod locomotor performance in both phenotypes of mice ($F_{1,24} = 19.41$, $P < 0.001$) as assessed by decreased latency (in seconds) to fall down from elevated rotarod. (*C* and *D*) Open-field locomotion data: MPTP produced a significant reduction in vertical and horizontal activity in the cKO mice, but not in the Het mice. Two-way ANOVA revealed significant treatment main effect (*C*, $F_{1,28} = 8.94$, $P < 0.01$; *D*, $F_{1,28} = 6.82$, $P < 0.05$), genotype main effect (*C*, $F_{1,28} = 6.12$, $P < 0.05$; *D*, $F_{1,28} = 0.08$, $P > 0.05$), and treatment × genotype interaction (*C*, $F_{1,28} = 4.31$, $P < 0.05$; *D*, $F_{1,28} = 0.235$, $P > 0.05$). (*E*) Elevated plus-maze test: MPTP significantly decreased risk-exploring behavior in the open arms in the cKO mice (treatment, $F_{1,20} = 4.76$, $P < 0.05$; genotype, $F_{1,20} = 0.1$, $P > 0.05$; treatment × phenotype interaction, $F_{1,20} = 1.57$, $P > 0.05$) as assessed by increased time spent in the closed arms (*$P < 0.05$, **$P < 0.01$, and ***$P < 0.001$ vs. saline solution group or Het control mice; *SI Appendix*, Fig. S4).

Given that depression and anxiety are nonmotor symptoms frequently reported by patients with PD (20), we tested the effects of MPTP on anxiety-like behavior by using the elevated plus-maze test. In VgluT2-cKO mice, MPTP treatment produced a significant increase in the time spent in the closed arms (Fig. 3*E*), an effect that was not observed after MPTP treatment in the VgluT2-Het control mice. These data suggest that selective deletion of VgluT2 in DA neurons also results in more severe anxiety-like behaviors after MPTP administration.

Deletion of VgluT2 in DA Neurons Did Not Alter MPTP-Induced Release of Apoptotic Factors. It was reported that MPTP-induced cell death may be result from elevated release of proapoptotic factors such as BAX and BAK and/or through reduced release of antiapoptotic factors such as Bcl-2 and Bcl-xL (21). To determine whether knocking out VgluT2 from DA neurons alters MPTP-induced changes in BAX and/or Bcl-2 production, thereby augmenting DA toxicity in VgluT2-cKO mice, we used Western blot assays to measure brain tissue levels of BAX and Bcl-2 at 14 d after saline solution or MPTP treatment. Compared with saline solution, MPTP treatment significantly decreased Bcl-2 expression in the striatum and increased BAX expression in the midbrain (*SI Appendix*, Fig. S4). However, no significant difference in Bcl-2 or BAX levels was observed between the two genotypes of mice, suggesting that enhanced toxicity of MPTP in VgluT2-cKO mice may be not related to altered production of the proapoptotic/antiapoptotic factors.

Deletion of VgluT2 in DA Neurons Decreases BDNF Expression in DA Neurons. It is well documented that neurotrophic factors, such as BDNF and/or glial-derived neurotrophic factor (GDNF), are DA neuron-protective in animal models of PD (22–24). In addition, recent studies indicate that glutamate release from presynaptic terminals promotes BDNF release from postsynaptic target cells in the cerebral cortex and hippocampus (25–27). BDNF, in turn, modulates local synaptic activity, development, and plasticity, as well as neuronal growth and survival (25–28). Given that glutamatergic neurons within the VTA may form synapses with DA neurons and functionally modulate DA neuronal activity (29, 30), we hypothesized that reduced glutamate release from DA neurons may decrease BDNF expression and release within the VTA/SNc and therefore decrease intrinsic resistance of DA neurons to MPTP toxicity. To test this hypothesis, we examined whether VgluT2 deletion in DA neurons alters the expression of BDNF, GDNF, and the BDNF receptor TrkB in DA neurons by using highly sensitive RNAscope ISH. High densities of BDNF mRNA were detected in the VTA and SNc, but not in the striatum (*SI Appendix*, Fig. S5*A*), whereas GDNF was detected mainly in the striatum, but not in the VTA or SNc (*SI Appendix*, Fig. S5*B*). Strikingly, VgluT2-cKO mice displayed a significant reduction in BDNF and TrkB mRNA expression in the VTA and SNc compared with the VgluT2-Het control mice (Fig. 4 and *SI Appendix*, Fig. S6).

We next examined the identity of BDNF-expressing neurons in the VTA and SNc. In VgluT2-Het control mice, approximately one third of TH^+ DA neurons expressed BDNF mRNA (Fig. 4 *A* and *C*) and ~50% of TH^+ DA neurons expressed TrkB (Fig. 4 *E* and *F*) in the VTA and SNc. Strikingly, there was a ~30–70% reduction in the number of $BDNF^+$-TH^+ cells (Fig. 4*C*), $TrkB^+$-TH^+ cells (Fig. 4*F* and *SI Appendix*, Fig. S6), or $BDNF^+$-$TrkB^+$-TH^+ cells (Fig. 4*G*) in VgluT2-cKO mice compared

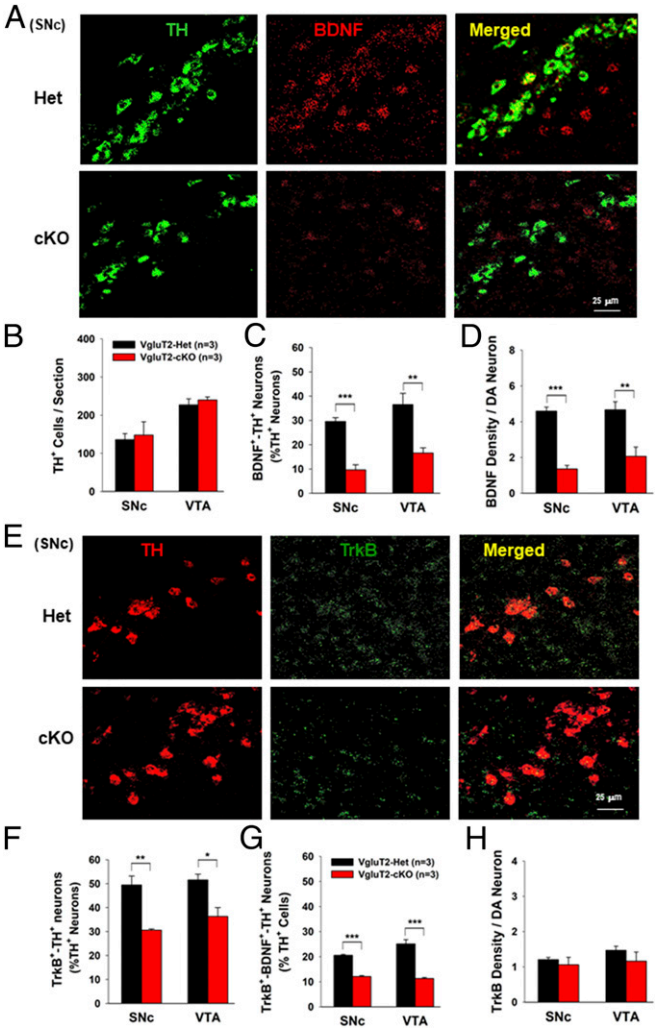

Fig. 4. Selective deletion of VgluT2 in DA neurons decreases BDNF/TrkB mRNA expression in DA neurons. (*A*) Representative confocal images in the SNc show a significant reduction in BDNF mRNA expression in cKO mice. (*B*) Mean TH^+ cell counts per section in the SNc and VTA. (*C*) The mean $BDNF^+$-TH^+ cell counts (percentage of total TH^+ cells) illustrate a ∼50% reduction in cKO mice compared with Het control mice (SNc, $t = 9.05$, $P < 0.001$; VTA, $t = 3.9$, $P < 0.01$). (*D*) BDNF density per DA neuron illustrates a significant reduction in BDNF density in DA neurons in the cKO mice (SNc, $t = 11.00$, $P < 0.001$; VTA, $t = 3.80$, $P < 0.01$). (*E*) Representative confocal images of TrkB mRNA staining in the SNc. (*F*) Mean $TrkB^+$-TH^+ cell counts (percentage of total TH^+ DA neurons) in the SNc and VTA show a significant decrease in $TrkB^+$-TH^+ cells in cKO mice (SNc, $t = 5.0$, $P < 0.01$; VTA, $t = 3.48$, $P < 0.05$). (*G*) The mean $TrkB^+$-$BDNF^+$-TH^+ cell counts (percentage of total TH^+ cells) show a significant reduction in cKO mice compared with Het control mice (SNc, $t = 16.93$, $P < 0.001$; VTA, $t = 7.84$, $P < 0.001$). (*H*) TrkB density per DA neuron shows a nonsignificant difference between the two groups of mice (SNc, $t = 0.66$, $P > 0.05$; VTA, $t = 027$, $P > 0.05$; $*P < 0.05$, $**P < 0.01$, and $***P < 0.001$ vs. Het control mice; *SI Appendix*, Figs. S5–S7).

with VgluT2-Het control mice. In addition, the VgluT2 deletion in DA neurons also significantly lowered the density of BDNF (Fig. 4*D*), but not TrkB (Fig. 4*H*), in DA neurons of cKO mice. We also examined the TrkB expression in surviving DA neurons after MPTP treatment. The remaining DA neurons showed a significantly higher expression of TrkB in DA neurons compared with that seen in saline solution control mice (*SI Appendix*, Fig. S7). These findings provide additional evidence supporting the neuroprotective role of BDNF-TrkB in DA neurons. Again, we did not see a significant difference in the total number of TH^+ DA neurons between the two genotypes of mice (Fig. 4*B*), suggesting that reduced BDNF expression in a small population of DA neurons does not significantly alter DA neuron survival in the absence of insults, but may contribute to the enhanced vulnerability of DA neurons to MPTP in VgluT2-cKO mice.

VgluT2 Overexpression in DA Neurons Restores BDNF/TrkB Expression in VgluT2-cKO Mice. To confirm a central role for VgluT2 expression in shaping DA neuron vulnerability to MPTP, and to further explore the potential link between VgluT2 expression and local BDNF/TrkB expression, we used viral approaches to rescue VgluT2 expression in DA neurons of VgluT2-cKO mice (*SI Appendix*, Fig. S8 *A* and *B*). Mice were injected with an AAV-DIO-VgluT2-GFP (AAV-VgluT2) viral vector or a control AAV-DIO-GFP (AAV-GFP) vector to drive expression of VgluT2 or GFP, respectively, within DAT-cre–expressing cells in VgluT2-cKO mice. Four weeks after bilateral AAV-VgluT2 injections into the VTA, VgluT2-GFP signal was detected in the majority (∼90%) of TH^+ DA neurons in the VTA and SNc (*SI Appendix*, Fig. S8 *C* and *D*), suggesting successful VgluT2 overexpression in DA neurons of VgluT2-cKO mice.

To confirm functional expression of VgluT2 within DA neurons in VgluT2-cKO mice, we microinjected a combination of AAV-DIO-VgluT2-GFP and AAV-DIO-ChR2-EYFP viral vectors. Eight weeks later, we performed whole-cell patch-clamp recordings of NAc MSNs combined with optical stimulation of VTA DA neuron terminals. Optogenetically evoked ESPCs were detected in 16 of 16 NAc MSNs in VgluT2-rescued mice ($n = 3$; *SI Appendix*, Fig. S8 *E* and *F*). These EPSCs were blocked by DNQX ($n = 6$ cells, three mice, paired t test, $P < 0.01$; *SI Appendix*, Fig. S8*G*) and showed comparable latency from laser onset to current onset, amplitude, and effectiveness of DNQX block to optogenetically evoked EPSCs recorded from VgluT2-Het mice (*SI Appendix*, Fig. S8 *H–J*). These electrophysiological findings confirm that this viral rescue strategy resulted in functional VgluT2 expression in DA neurons and restored glutamate release from DA neuron terminals in the NAc of VgluT2-cKO mice

To determine whether the resultant VgluT2 overexpression can restore the BDNF/TrkB expression in midbrain DA neurons in VgluT2-rescued mice, we examined the BDNF/TrkB gene expression in the SNc and VTA by using RNAscope (Fig. 5*A*). The AAV-DIO-VgluT2 vector injections did not alter total TH^+ cell counts in the SNc or VTA of VgluT2-cKO mice (Fig. 5*B*), but significantly increased the BDNF and TrkB expression in DA neurons in the SNc and VTA in VgluT2-cKO mice (Fig. 5). Importantly, rescued VgluT2 expression restored BDNF expression back to ∼30% of DA neurons (Fig. 5*C*) and TrkB expression back to ∼60% of DA neurons (Fig. 5*F*). Rescued VgluT2 expression in VgluT2-cKO mice also restored the BDNF and TrkB coexpression in DA neurons (Fig. 5*G*) and increased the density of BDNF (Fig. 5*D*), but not TrkB (Fig. 5*H*), in $BDNF^+$ or $TrkB^+$ cells. These findings suggest that the VgluT2 expression in DA neurons modulates expression of BDNF and TrkB in a subpopulation of DA neurons.

VgluT2 Overexpression in DA Neurons Prevents MPTP-Induced DA Neurotoxicity and Behavioral Impairment. We next examined the effects of VgluT2 overexpression on MPTP-induced toxicity in VgluT2-cKO mice (Fig. 6 *A* and *B*). Following saline solution treatment, there was no difference in the number of TH^+ cells within the SNc or VTA of VgluT2-cKO mice injected with AAV-GFP or AAV-VgluT2 virus. MPTP treatment produced significant loss of TH^+ DA neurons in the SNc and VTA of both groups of mice (Fig. 6 *A–C*). However, this loss was significantly attenuated in VgluT2-cKO mice injected with AAV-VgluT2 virus (Fig. 6 *A–C*), with protection being particularly prominent in the SNc (Fig. 6*C*).

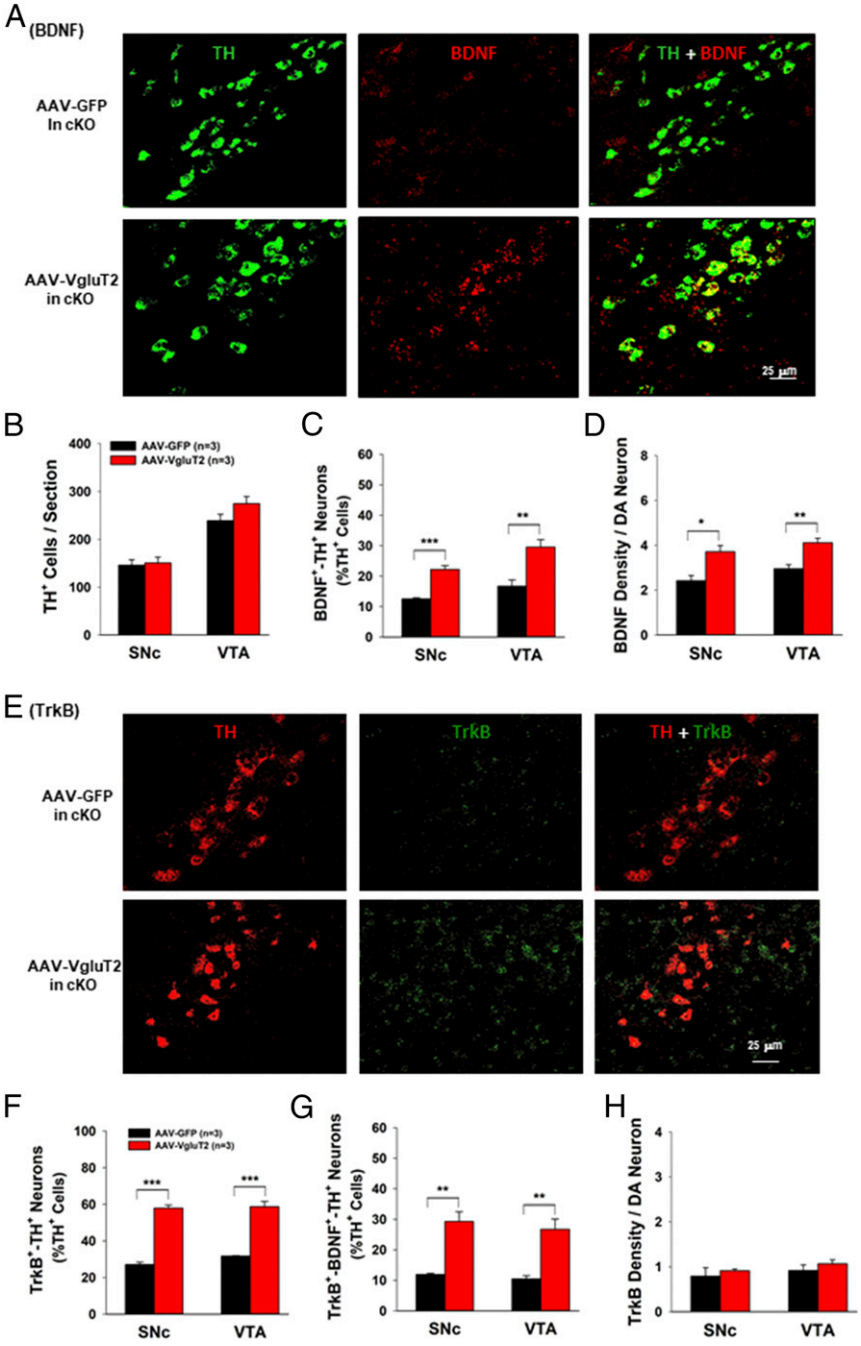

Fig. 5. Viral rescue of VgluT2 expression in VgluT2-cKO mice restored BDNF/TrkB expression in DA neurons. (*A*) Representative confocal images in the SNc illustrates BDNF expression in VgluT2-overexpressing mice. (*B*) Quantitative data illustrate that VgluT2 overexpression did not alter total numbers of TH^+ DA neurons. (*C*) VgluT2 overexpression significantly increased the cell counts of $BDNF^+$-TH^+ neurons (SNc, $t = 7.54$, $P < 0.001$; VTA, $t = 3.96$, $P < 0.01$). (*D*) VgluT2 overexpression significantly increased BDNF density per DA neuron (SNc, $t = 3.57$, $P < 0.05$; VTA, $t = 4.32$, $P < 0.01$). (*E*) Representative confocal images of TrkB mRNA staining in the SNc. (*F*) Quantitative data illustrate that the VgluT2 overexpression significantly increased TrkB expression in TH^+ DA neurons (SNc, $t = 14.8$, $P < 0.001$; VTA, $t = 9.53$, $P < 0.001$). (*G*) VgluT2 overexpression also significantly increased the cell counts of $TrkB^+$-$BDNF^+$-TH^+ neurons (SNc, $t = 5.4$, $P < 0.01$; VTA, $t = 4.65$, $P < 0.01$). (*H*) VgluT2 overexpression did not alter TrkB density in DA neurons (SNc, $t = 0.33$, $P > 0.05$; VTA, $t = 0.44$, $P > 0.05$; $^*P < 0.05$, $^{**}P < 0.01$, and $^{***}P < 0.001$ vs. AAV-GFP control mice).

We also assessed locomotor function in VgluT2-cKO mice injected with AAV-GFP or AAV-VgluT2 virus. Consistent with histological findings regarding DA neuron toxicity, VgluT2 overexpression in DA neurons significantly attenuated MPTP-induced locomotor impairment, as assessed by the parallel rod floor test (Fig. 6*D*), the rotarod test (Fig. 6*E*), and open-field locomotion (Fig. 6 *F* and *G*).

Discussion

The major findings of the present study are that (*i*) selective deletion of the VgluT2 gene in midbrain DA neurons significantly decreased BDNF/TrkB expression in a subpopulation of DA neurons and increased the DA neuron vulnerability to the neurotoxin MPTP in VgluT2-cKO mice and (*ii*) viral rescue of VgluT2 expression in DA neurons in VgluT2-cKO mice restored

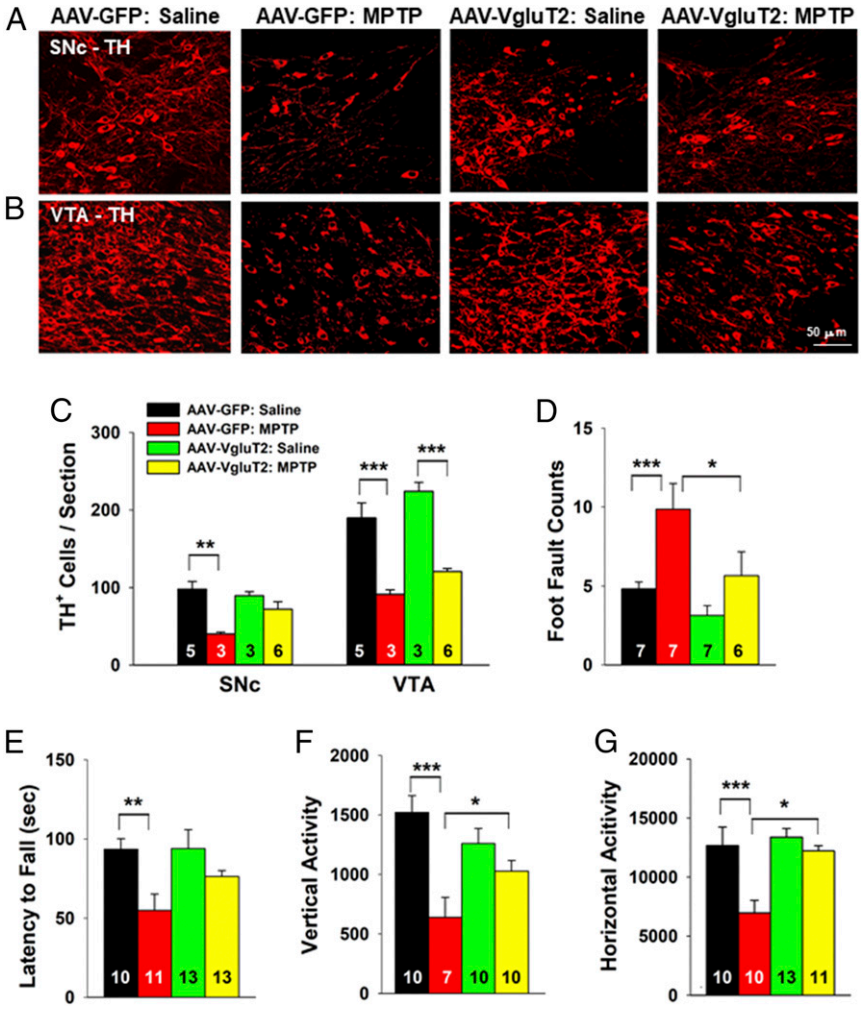

Fig. 6. Viral rescue of VgluT2 expression in DA neurons in VgluT2-cKO mice attenuated MPTP-induced DA neuron toxicity and locomotor impairment. (*A* and *B*) TH immunostaining in the SNc and VTA. (*C*) Mean TH^+ cell counts per section. MPTP produced more DA cell loss in the AAV-GFP control mice than in the VgluT2-rescued mice (SNc, $F_{3,13} = 6.43$, $P < 0.01$; VTA, $F_{3,13} = 17.88$, $P < 0.001$, one-way ANOVA). (*D* and *E*) MPTP produced a significant increase in foot fault counts (*D*, one-way ANOVA, $F_{3,23} = 10.73$, $P < 0.001$) and a significant decrease in rotarod performance (*E*, $F_{3,43} = 4.74$, $P < 0.01$) in the AAV-GFP control mice but not in VgluT2-overexpressing mice. (*F* and *G*) Viral rescue of VgluT2 expression attenuated MPTP-induced reduction in vertical (F, $F_{3,33} = 8.41$, $P < 0.001$) and horizontal (*G*, $F_{3,40} = 8.87$, $P < 0.001$) locomotor activity (*$P < 0.05$, **$P < 0.01$, and ***$P < 0.001$ between groups labeled by horizontal bars; *SI Appendix*, Fig. S8)

BDNF/TrkB expression in DA neurons and attenuated MPTP-induced DA neuron toxicity and locomotor impairment. These findings suggest that VgluT2 expression in DA neurons of the adult brain is neuroprotective against neurotoxin-induced DA neuron degeneration. Moreover, these findings raise the possibility that genetic or environmental factors causing reduced expression or function of VgluT2 in DA neurons may place some individuals at increased risk for DA neuron degeneration. Accordingly, renormalization of, or increase in, VgluT2 expression in DA neurons may represent a promising therapeutic approach for treatment of PD or other neurodegenerative diseases.

PD is the second most common neurodegenerative disease after Alzheimer's disease. The molecular mechanisms underlying DA neuron degeneration in PD are still poorly understood. Extensive research indicates that mitochondrial dysfunction caused by complex I impairment and oxidative stress may render DA neurons vulnerable to excitotoxicity in PD (31, 32). The interaction of genetic and environmental risk factors has been a major focus in PD research. Gene mutations in several functional proteins such as leucine-rich repeat kinase 2 (LRRK2), α-synuclein, parkin, and DJ-1 (PARK7 protein gene) have been associated with rare inherited forms of PD or DA neuron dysfunction and degeneration (33–36). However, there is at present no direct evidence that any of these genes have a direct role in the etiology of the common sporadic form of PD, suggesting that other unknown mechanisms may be involved.

It was reported that postmortem brain tissues of patients with PD exhibited significant alterations in vesicular glutamate transporter expression in the cortex and striatum, suggesting possible involvement of vesicular glutamate transporters in PD (37, 38). Three vesicular glutamate transporters (VgluT1–3) were identified. VgluT1 and VgluT2 are responsible for the uploading of glutamate into synaptic vesicles and were the first specific markers of glutamatergic neurons identified (18). VgluT1 is expressed in glutamatergic neurons mainly in cortex and hippocampus, whereas VgluT2 is expressed in glutamatergic neurons mainly in subcortical brain regions, including the thalamus, VTA, and SNc (11, 18). Recent studies suggest that VgluT2 is also expressed in a subpopulation of DA neurons and functionally modulates DA and glutamate corelease from $VgluT2^+$-TH^+ neurons (39–41). VgluT2 has been generally believed to promote glutamate loading into synaptic glutamate

vesicles (9, 42). However, recent studies indicate that VgluT2 also promotes DA loading into the vesicles by increasing the vesicular pH gradient (or vesicular hyperacidification), thereby promoting vesicular DA loading (13, 43). In the present study, we found that ~20% of DA neurons in the VTA and SNc coexpress VgluT2, which mediates glutamate release from DA neurons in VgluT2-Het control mice. VgluT2-cKO mice showed a substantial reduction in VgluT2-TH– or VgluT2-DAT–coexpressing neurons (from ~20% to <5%).

Electrophysiological evidence indicates that selective deletion of VgluT2 completely eliminated glutamate release from DA neurons evoked by photoactivation of terminals from VTA DA neurons. These findings are in agreement with previous reports (15, 41, 44). Given the important role of DA and glutamate in reward and locomotion (2, 45), most recent studies have focused on the functional role of VgluT2 coexpression in locomotion and psychostimulant action. In the present study, we found that genetic deletion of VgluT2 in DA neurons did not significantly alter basal levels of locomotor activity or locomotor performance in multiple behavioral tests. Consistent with these findings, we also did not see significant changes in total TH^+ or DAT^+ cell counts and striatal TH density in the absence of insults. Similarly, deletion of VgluT2 in catecholaminergic neurons in the rostral ventrolateral medulla also failed to alter neuronal cell counts and survival in VgluT2-cKO mice (46, 47). These results are consistent with previous reports that there is no significant difference in basal locomotor activity or striatal DA content observed between the two genotypes of mice (12, 13), but contrast with another report indicating that VgluT2-cKO mice displayed a significant reduction in TH^+ cell count and basal level of locomotion compared with WT control mice (15). Behavioral and synaptic responses to psychostimulants are generally reported to be blunted in VgluT2-cKO mice (12, 13, 15, 48), although there are examples to the contrary (14, 49). The reasons for conflicting findings in basal and psychostimulant-evoked function are unclear.

In the present study, we found that selective deletion of VgluT2 in DA neurons significantly increased vulnerability of DA neurons to the neurotoxin MPTP, which could, moreover, be prevented by overexpression of VgluT2 in DA neurons in VgluT2-cKO mice. In Het and cKO mice, not all DA neurons are killed by the MPTP treatment regimen (50) used in this study. Strikingly, in Het mice, a greater percentage of surviving DA neurons displayed VgluT2 expression after MPTP treatment, providing additional evidence that VgluT2-expressing neurons are better able to survive neurotoxic insults. Given that VgluT2-expressing DA neurons are also present in nonhuman primates and humans (51), our finding suggests that loss of, or reduced, VgluT2 expression in a small population of DA neurons may constitute a new risk factor in the development of DA neurodegeneration and PD. Accordingly, restoration of VgluT2 expression in DA neurons may represent a new therapeutic strategy for treatment of PD or other neurodegenerative diseases.

It is unknown how VgluT2 deletion in DA neurons increases vulnerability to MPTP. Studies in cortex and hippocampus have found that glutamate release from presynaptic terminals promotes release of the neurotrophin BDNF from target cells in Ca^{2+}-dependent and neuronal activity-dependent manners (25–27, 52, 53). Pharmacological activation of AMPA receptors also promotes BDNF expression in cerebral cortex (54). BDNF, in turn, modulates local synaptic activity, development, and plasticity, as well as neuronal growth and survival by activation of TrkB receptors (25–28). Given that VgluT2-expressing glutamate neurons within the VTA may form functional synapses with VTA DA neurons (29, 30), we propose that this glutamate-mediated BDNF release may also occur in the VTA/SNc in healthy subjects. Specifically, glutamate release from VgluT2-expressing DA neurons may promote BDNF synthesis and release in the VTA/SNc, which subsequently modulates DA neuron growth and survival by activation of TrkB (25, 55). Accordingly, reduced glutamate release from DA neurons in VgluT2-cKO mice would decrease BDNF/TrkB expression in VTA or SNc neurons, thereby decreasing neuronal resilience to MPTP. Therefore, it is reasonable to hypothesize that reduced BDNF/TrkB expression in a subpopulation of DA neurons could be the result after VgluT2 deletion that abolishes glutamate release from DA neurons during development in embryonic and postnatal stages. This hypothesis is supported by several lines of evidence: (*i*) BDNF is DA neuron-protective in animal models of PD (22–24) and (*ii*) there are ~20% of DA neurons that express VgluT2, ~30% of DA neurons that coexpress BDNF, and ~50% of DA neurons that coexpress TrkB. In addition, ~20% of DA neurons coexpressed BDNF and TrkB, suggesting that the BDNF-TrkB signal system plays an important role in protecting a subpopulation of midbrain DA neurons. (*iii*) Deletion of VgluT2 caused a significant reduction in BDNF and TrkB expression in DA neurons, matching well in the extent of damage with the findings of DA neuronal loss in VgluT2-cKO mice after MPTP administration; and (*iv*) restoration of VgluT2 expression in DA neurons restored glutamate release from VgluT2-rescued DA neurons and also restored BDNF and TrkB expression in DA neurons. These findings suggest the presence of an endogenous VgluT2-glutamate-BNDF-TrkB signal system that protects a subpopulation of TrkB-expressing DA neurons. Previous studies indicate that BDNF expression is decreased in the SNc of postmortem brains, and in the cerebrospinal fluid, of patients with PD (56, 57), as well as in animal models of PD (58). However, the phenotypes of cells that express BDNF in these previous reports are unknown. It is also unknown whether this decrease in BDNF is a consequence of DA neuron loss in PD or a cause of DA neuron degeneration in PD. The present findings indicate that decreased BDNF/TrkB expression in DA neurons may be an important risk factor leading to DA neuron degeneration in PD. We note that VgluT2 overexpression did not completely block MPTP-induced DA neuron toxicity, suggesting that other non–BDNF-TrkB mechanisms may be involved. In our experimental approach, VgluT2 is removed from DA neurons in early postnatal development. Although we cannot exclude the possibility that this developmental alteration causes subtle changes in maturation that increases vulnerability of these neurons, our viral overexpression experiments argue that VgluT2 expression is a key factor shaping resilience of DA neurons to toxic insults in adult mice. Regardless, the present findings suggest that VgluT2 expression in a small population of DA neurons is critical in protecting DA neurons against environmental toxins or insults in a BDNF-TrkB–associated manner.

In summary, by using conditional VgluT2-KO techniques, we found that deletion of VgluT2 in a subpopulation of DA neurons abolished glutamate release from these cells, causing a reduction in BDNF and TrkB expression in midbrain DA neurons and an increase in vulnerability to MPTP-induced DA cell death and locomotor impairment. Restoration of VgluT2 expression in VgluT2-cKO mice normalized BDNF/TrkB expression and attenuated MPTP-induced toxicity in DA neurons and locomotor dysfunction. These findings suggest that reduced VgluT2 expression in DA neurons may be a newly identified risk factor in the development of neurodegenerative diseases such as PD, and normalization of VgluT2 expression in DA neurons may be useful in preventing and treating PD or other neurodegenerative diseases.

Materials and Methods

Animals. Male adult VgluT2-cKO mice ($VgluT2^{flox/flox;DAT\text{-}Cre+/-}$) and their heterozygous littermates ($VgluT2^{flox/-;DAT\text{-}Cre+/-}$), aged 8–12 wk, were used in all behavioral experiments and were maintained on a 12-h light/dark cycle

with food and water available ad libitum. All experimental procedures were conducted in accordance with the *Guide for the Care and Use of Laboratory Animals* of the US National Research Council (59) and approved by the animal care committee of the National Institute on Drug Abuse of the National Institutes of Health. Complete descriptions of experimental animals are provided in *SI Appendix, Experimental Procedures*.

Intracranial Microinjection Surgeries. For intra-VTA microinjection of viruses, male mice were anesthetized with sodium pentobarbital (60 mg/kg i.p.) and placed in a stereotaxic frame (David Kopf Instruments). Complete microinjection methods are described in *SI Appendix, Experimental Procedures*.

Behavioral Tests. Behavioral tests, including open-field locomotion, rotarod test, parallel rod floor test, and elevated plus maze, were carried out from day 14 after MPTP (18 mg/kg × 4 with 2-h interinjection intervals; Sigma–Aldrich) or saline solution injections in mice without intracranial AAV injections or 4 wk after intracranial AAV-VgluT2 microinjections. Complete experimental methods for these four behavioral tests are described in *SI Appendix, Experimental Procedures*.

Electrophysiology. Electrophysiological recordings began 8–10 wk after the viral vector injections as described previously (60). Briefly, animals were anesthetized and perfused with ice-cold artificial cerebrospinal fluid (ACSF). Brains were cut into 200-μm coronal sections in ice-cold ACSF. Tissue was recovered for 10 min at 32 °C and then held in standard ACSF for at least 60 min before recording. Complete descriptions of electrophysiological recordings are provided in *SI Appendix, Experimental Procedures*.

Western Blotting. Western blot analysis was performed as reported previously (61). Mice were perfused transcardially with cold 0.9% saline solution under deep anesthesia. Whole striatum and midbrain containing the VTA and SNc were dissected. Tissues were homogenized in RIPA lysis buffer (Cell Signaling Technology), and the protein concentration for each sample was quantified with a Bio-Rad Protein Assay. Complete descriptions of Western blotting methods are provided in *SI Appendix, Experimental Procedures*.

Immunohistochemistry Assays. Mice were deeply anesthetized and perfused transcardially with cold 0.9% (wt/vol) saline solution followed by 4% (vol/vol) paraformaldehyde in 0.1 M phosphate buffer. Brain tissues were then transferred to 20% (wt/vol) sucrose in phosphate buffer at 4 °C overnight. Coronal sections were cut at 25 μm on a cryostat (CM3050S; Leica Microsystems), and every fourth section was collected. Tissue sections containing the striatum or VTA/SNc were blocked and floated in 4% (wt/vol) BSA and 0.3% (vol/vol) Triton X-100 phosphate buffer for 2 h at room temperature. Immunohistochemistry was then performed by using mouse anti-TH monoclonal antibody (1:500; Millipore) that recognizes the extracellular N terminus of TH or mouse anti-VgluT2 monoclonal antibody (1:500; cat. no. MAB5504; Millipore). After washing, sections were further incubated with a mixture of secondary antibodies: Alexa Fluor 488 donkey anti-mouse IgG for TH (1:500) in 4% BSA and 0.3% Triton X-100 phosphate buffer for 2 h at room temperature. Sections were then washed, mounted, and coverslipped. Fluorescent images were obtained with a FV1000 confocal fluorescence microscope system (Olympus). All images were taken and presented under identical optical conditions. TH^+ neurons in the VTA and SNc were counted in six stereologically selected sections per brain with 100-μm spacing between sections from the rostral to the caudal level under 20× magnification (62). Densitometric analysis followed similar methods as choosing a section to quantify TH immunostaining density on individual brain slices containing striatum with the use of ImageJ software (61, 63). The TH^+ cell counting and TH immunostaining analyses were conducted in a double-blinded manner.

RNAscope ISH. RNAscope ISH was used to detect cell type-specific expression of VgluT2 mRNA, TH mRNA, DAT mRNA, BDNF mRNA, GDNF mRNA, or TrkB mRNA. Mice were deeply anesthetized, and the whole brain was removed and rapidly frozen on dry ice. Fresh-frozen tissue sections (14 μm thick) were mounted on positively charged microscopic glass slides (Fisher Scientific) and stored at −80 °C until RNAscope ISH assays were performed. Multiple target gene-specific RNAscope probes were used to observe the cellular distributions of VgluT2, TH, DAT, BDNF, TrkB, or GDNF mRNA in the striatum, VTA, or SNc by using a VgluT2 RNAscope probe (Mm-Slc17a6-C2-Vglut-2 probe; cat. no. 319171-C2; targeting 1,986–2,998 bp of the *Mus musculus* VgluT2 mRNA sequence, NM_080853.3), TH RNAscope probe (Mm-Th-C2; cat. no. 317621-C2; targeting 483–1,603 bp of the *M. musculus* TH mRNA sequence, NM_009377.1), BDNF-specific RNAscope probe (Mm-Bdnf-CDS-C3-BDNF probe; cat. no. 457761-C3; targeting 662–1,403 bp of the *M. musculus* BDNF mRNA sequence, NM_007540.4), TrkB RNAscope probe [Mm-Ntrk2-C1; cat. no. 423611; targeting 668–1,582 bp of *M. musculus* neurotrophic tyrosine kinase receptor type 2 (Ntrk2), transcript variant 2, mRNA sequence], GDNF RNAscope probe (Mm-Gdnf-3UTR-GDNF; cat. no. 421941-C2; targeting 12–765 bp of the *M. musculus* GDNF mRNA sequence NM_010275.2), and DAT RANscope (Mm-Slc6a3-C2; cat. no. 315441; targeting 1,486–2,525 bp of the *M. musculus* solute carrier family 6 DAT mRNA sequence). All these probes were designed and provided by Advanced Cell Diagnostics. The RNAscope mRNA assays were performed following the manufacturer's protocols. Stained slides were coverslipped with fluorescent mounting medium (ProLong Gold anti-fade reagent P36930; Life Technologies) and scanned into digital images with an Olympus FluoView FV1000 confocal microscope at 40× or 60× magnification with the use of manufacturer-provided software. Cells expressing TH mRNA, DAT mRNA, VgluT2 mRNA, BDNF mRNA, or both transcripts in the VTA and SNc were counted in a double-blinded manner in six stereologically selected sections per brain with 64-μm spacing between sections from the rostral to the caudal level under 40× magnification (62).

Image Analysis. All microscope and camera settings (i.e., light level, exposure, gain) were identical for all acquired images. Postprocessing of all immunohistochemistry and ISH images was performed by using ImageJ software (version 1.45s; https://imagej.nih.gov/ij/). For the cell counting and density analyses, the threshold of the function was applied to all images as we reported previously (64) so no bias was introduced by the software.

Data Analysis. All data are presented as mean ± SEM. Statistically significant differences were analyzed by *t* test, one-way ANOVA, or two-way ANOVA as appropriate. All raw data in DA cell counts or density measurements met the criteria for normal distribution. The statistical results of the ANOVA were reported by using the notation $F_{a,b}$ values (*a* degree of freedom refers to the number of grouping levels minus 1, and *b* degree of freedom refers to the total number of observations minus the total number of groups), and *P* values are reported in *Results* and/or figure legends. Post hoc individual group comparisons were carried out by Student–Newman–Keuls method. Statistical significance was defined at $P < 0.05$.

ACKNOWLEDGMENTS. We thank Haiying Zhang and Yi He [National Institute on Drug Abuse (NIDA) Intramural Research Program (IRP)] for their help with RNAscope ISH experiments; Carlos Mejias-Aponte (Image Core Facility, NIDA IRP) for help in slicing part of the brains; the NIDA breeding staff for breeding the transgenic animals; and Stephanie Gantz, Chloe Jordan, and Wendy Xin (NIDA IRP) for their critical reading of the manuscript. This research was supported by NIDA intramural research programs.

1. Sgambato-Faure V, Tremblay L (2018) Dopamine and serotonin modulation of motor and non-motor functions of the non-human primate striato-pallidal circuits in normal and pathological states. *J Neural Transm (Vienna)* 125:485–500.
2. Palmiter RD (2008) Dopamine signaling in the dorsal striatum is essential for motivated behaviors: Lessons from dopamine-deficient mice. *Ann N Y Acad Sci* 1129: 35–46.
3. Damier P, Hirsch EC, Agid Y, Graybiel AM (1999) The substantia nigra of the human brain. II. Patterns of loss of dopamine-containing neurons in Parkinson's disease. *Brain* 122:1437–1448.
4. Jabre M, Nohra G, Damier P, Bejjani BP (2008) Does dopamine still have a leading role in advanced Parkinson's disease after subthalamic stimulation? *Stereotact Funct Neurosurg* 86:184–186.
5. Chaudhuri KR, Schapira AH (2009) Non-motor symptoms of Parkinson's disease: Dopaminergic pathophysiology and treatment. *Lancet Neurol* 8:464–474.
6. Drui G, et al. (2014) Loss of dopaminergic nigrostriatal neurons accounts for the motivational and affective deficits in Parkinson's disease. *Mol Psychiatry* 19:358–367.
7. Bérubé-Carrière N, et al. (2009) The dual dopamine-glutamate phenotype of growing mesencephalic neurons regresses in mature rat brain. *J Comp Neurol* 517: 873–891.
8. Chuhma N, Choi WY, Mingote S, Rayport S (2009) Dopamine neuron glutamate cotransmission: Frequency-dependent modulation in the mesoventromedial projection. *Neuroscience* 164:1068–1083.
9. Morales M, Margolis EB (2017) Ventral tegmental area: Cellular heterogeneity, connectivity and behaviour. *Nat Rev Neurosci* 18:73–85.
10. Trudeau LE, et al. (2014) The multilingual nature of dopamine neurons. *Prog Brain Res* 211:141–164.
11. Morales M, Root DH (2014) Glutamate neurons within the midbrain dopamine regions. *Neuroscience* 282:60–68.

12. Birgner C, et al. (2010) VGLUT2 in dopamine neurons is required for psychostimulant-induced behavioral activation. *Proc Natl Acad Sci USA* 107:389–394.
13. Hnasko TS, et al. (2010) Vesicular glutamate transport promotes dopamine storage and glutamate corelease in vivo. *Neuron* 65:643–656.
14. Alsiö J, et al. (2011) Enhanced sucrose and cocaine self-administration and cue-induced drug seeking after loss of VGLUT2 in midbrain dopamine neurons in mice. *J Neurosci* 31:12593–12603.
15. Fortin GM, et al. (2012) Glutamate corelease promotes growth and survival of midbrain dopamine neurons. *J Neurosci* 32:17477–17491.
16. Jackson-Lewis V, Przedborski S (2007) Protocol for the MPTP mouse model of Parkinson's disease. *Nat Protoc* 2:141–151.
17. Blesa J, Przedborski S (2014) Parkinson's disease: Animal models and dopaminergic cell vulnerability. *Front Neuroanat* 8:155.
18. Fremeau RT, Jr, Voglmaier S, Seal RP, Edwards RH (2004) VGLUTs define subsets of excitatory neurons and suggest novel roles for glutamate. *Trends Neurosci* 27:98–103.
19. Zörner B, et al. (2010) Profiling locomotor recovery: Comprehensive quantification of impairments after CNS damage in rodents. *Nat Methods* 7:701–708.
20. Hurt CS, et al.; PROMS-PD study group (2014) Motor phenotypes, medication and mood: Further associations with impulsive behaviours in Parkinson's disease. *J Parkinsons Dis* 4:245–254.
21. Ethell DW, Fei Q (2009) Parkinson-linked genes and toxins that affect neuronal cell death through the Bcl-2 family. *Antioxid Redox Signal* 11:529–540.
22. Porritt MJ, Batchelor PE, Howells DW (2005) Inhibiting BDNF expression by antisense oligonucleotide infusion causes loss of nigral dopaminergic neurons. *Exp Neurol* 192: 226–234.
23. Maswood N, et al. (2004) Caloric restriction increases neurotrophic factor levels and attenuates neurochemical and behavioral deficits in a primate model of Parkinson's disease. *Proc Natl Acad Sci USA* 101:18171–18176.
24. Levivier M, Przedborski S, Bencsics C, Kang UJ (1995) Intrastriatal implantation of fibroblasts genetically engineered to produce brain-derived neurotrophic factor prevents degeneration of dopaminergic neurons in a rat model of Parkinson's disease. *J Neurosci* 15:7810–7820.
25. Leal G, Bramham CR, Duarte CB (2017) BDNF and hippocampal synaptic plasticity. *Vitam Horm* 104:153–195.
26. Kuczewski N, Porcher C, Lessmann V, Medina I, Gaiarsa JL (2009) Activity-dependent dendritic release of BDNF and biological consequences. *Mol Neurobiol* 39:37–49.
27. Gottmann K, Mittmann T, Lessmann V (2009) BDNF signaling in the formation, maturation and plasticity of glutamatergic and GABAergic synapses. *Exp Brain Res* 199:203–234.
28. Wong YH, Lee CM, Xie W, Cui B, Poo MM (2015) Activity-dependent BDNF release via endocytic pathways is regulated by synaptotagmin-6 and complexin. *Proc Natl Acad Sci USA* 112:E4475–E4484.
29. Wang HL, Qi J, Zhang S, Wang H, Morales M (2015) Rewarding effects of optical stimulation of ventral tegmental area glutamatergic neurons. *J Neurosci* 35: 15948–15954.
30. Dobi A, Margolis EB, Wang HL, Harvey BK, Morales M (2010) Glutamatergic and nonglutamatergic neurons of the ventral tegmental area establish local synaptic contacts with dopaminergic and nondopaminergic neurons. *J Neurosci* 30:218–229.
31. Beal MF, Matthews RT, Tieleman A, Shults CW (1998) Coenzyme Q10 attenuates the 1-methyl-4-phenyl-1,2,3,tetrahydropyridine (MPTP) induced loss of striatal dopamine and dopaminergic axons in aged mice. *Brain Res* 783:109–114.
32. Mattson MP, Pedersen WA, Duan W, Culmsee C, Camandola S (1999) Cellular and molecular mechanisms underlying perturbed energy metabolism and neuronal degeneration in Alzheimer's and Parkinson's diseases. *Ann N Y Acad Sci* 893:154–175.
33. Gasser T (1999) [Current pharmacologic therapy of idiopathic Parkinson's syndrome]. *Internist (Berl)* 40:1228–1235.
34. Koros C, Simitsi A, Stefanis L (2017) Genetics of Parkinson's disease: Genotype-phenotype correlations. *Int Rev Neurobiol* 132:197–231.
35. Manzoni C (2017) The LRRK2-macroautophagy axis and its relevance to Parkinson's disease. *Biochem Soc Trans* 45:155–162.
36. Al-Rumayyan A, Klein C, Alfadhel M (2017) Early-onset parkinsonism: Case report and review of the literature. *Pediatr Neurol* 67:102–106.e1.
37. Chung EK, Chen LW, Chan YS, Yung KK (2006–2007) Up-regulation in expression of vesicular glutamate transporter 3 in substantia nigra but not in striatum of 6-hydroxydopamine-lesioned rats. *Neurosignals* 15:238–248.
38. Kashani A, Betancur C, Giros B, Hirsch E, El Mestikawy S (2007) Altered expression of vesicular glutamate transporters VGLUT1 and VGLUT2 in Parkinson disease. *Neurobiol Aging* 28:568–578.
39. Dal Bo G, et al. (2004) Dopamine neurons in culture express VGLUT2 explaining their capacity to release glutamate at synapses in addition to dopamine. *J Neurochem* 88: 1398–1405.
40. Yamaguchi T, Qi J, Wang HL, Zhang S, Morales M (2015) Glutamatergic and dopaminergic neurons in the mouse ventral tegmental area. *Eur J Neurosci* 41:760–772.
41. Kawano M, et al. (2006) Particular subpopulations of midbrain and hypothalamic dopamine neurons express vesicular glutamate transporter 2 in the rat brain. *J Comp Neurol* 498:581–592.
42. Zhang S, et al. (2015) Dopaminergic and glutamatergic microdomains in a subset of rodent mesoaccumbens axons. *Nat Neurosci* 18:386–392.
43. Aguilar JI, et al. (2017) Neuronal depolarization drives increased dopamine synaptic vesicle loading via VGLUT. *Neuron* 95:1074–1088.e7.
44. Mendez JA, et al. (2008) Developmental and target-dependent regulation of vesicular glutamate transporter expression by dopamine neurons. *J Neurosci* 28:6309–6318.
45. Kalivas PW, Volkow ND (2011) New medications for drug addiction hiding in glutamatergic neuroplasticity. *Mol Psychiatry* 16:974–986.
46. Wallén-Mackenzie A, et al. (2006) Vesicular glutamate transporter 2 is required for central respiratory rhythm generation but not for locomotor central pattern generation. *J Neurosci* 26:12294–12307.
47. Abbott SB, Holloway BB, Viar KE, Guyenet PG (2014) Vesicular glutamate transporter 2 is required for the respiratory and parasympathetic activation produced by optogenetic stimulation of catecholaminergic neurons in the rostral ventrolateral medulla of mice in vivo. *Eur J Neurosci* 39:98–106.
48. Adrover MF, Shin JH, Alvarez VA (2014) Glutamate and dopamine transmission from midbrain dopamine neurons share similar release properties but are differentially affected by cocaine. *J Neurosci* 34:3183–3192.
49. Wang DV, et al. (2017) Disrupting glutamate co-transmission does not affect acquisition of conditioned behavior reinforced by dopamine neuron activation. *Cell Rep* 18:2584–2591.
50. Meredith GE, Rademacher DJ (2011) MPTP mouse models of Parkinson's disease: An update. *J Parkinsons Dis* 1:19–33.
51. Root DH, et al. (2016) Glutamate neurons are intermixed with midbrain dopamine neurons in nonhuman primates and humans. *Sci Rep* 6:30615.
52. Reichardt LF (2006) Neurotrophin-regulated signalling pathways. *Philos Trans R Soc Lond B Biol Sci* 361:1545–1564.
53. Nikulina EM, Johnston CE, Wang J, Hammer RP, Jr (2014) Neurotrophins in the ventral tegmental area: Role in social stress, mood disorders and drug abuse. *Neuroscience* 282:122–138.
54. Clarkson AN, et al. (2011) AMPA receptor-induced local brain-derived neurotrophic factor signaling mediates motor recovery after stroke. *J Neurosci* 31:3766–3775.
55. Kuczewski N, Porcher C, Gaiarsa JL (2010) Activity-dependent dendritic secretion of brain-derived neurotrophic factor modulates synaptic plasticity. *Eur J Neurosci* 32: 1239–1244.
56. Mogi M, et al. (1999) Brain-derived growth factor and nerve growth factor concentrations are decreased in the substantia nigra in Parkinson's disease. *Neurosci Lett* 270:45–48.
57. Howells DW, et al. (2000) Reduced BDNF mRNA expression in the Parkinson's disease substantia nigra. *Exp Neurol* 166:127–135.
58. Nagatsu T, Sawada M (2005) Inflammatory process in Parkinson's disease: Role for cytokines. *Curr Pharm Des* 11:999–1016.
59. National Research Council (2011) *Guide for the Care and Use of Laboratory Animals* (National Academies Press, Washington, DC), 8th Ed.
60. McDevitt RA, et al. (2014) Serotonergic versus nonserotonergic dorsal raphe projection neurons: Differential participation in reward circuitry. *Cell Rep* 8:1857–1869.
61. Song R, et al. (2012) Increased vulnerability to cocaine in mice lacking dopamine D3 receptors. *Proc Natl Acad Sci USA* 109:17675–17680.
62. Wang HL, Morales M (2008) Corticotropin-releasing factor binding protein within the ventral tegmental area is expressed in a subset of dopaminergic neurons. *J Comp Neurol* 509:302–318.
63. Zhang HY, et al. (2014) Cannabinoid CB2 receptors modulate midbrain dopamine neuronal activity and dopamine-related behavior in mice. *Proc Natl Acad Sci USA* 111: E5007–E5015.
64. De Biase LM, et al. (2017) Local cues establish and maintain region-specific phenotypes of basal ganglia microglia. *Neuron* 95:341–356.e6.